Resonant emission of solitons from impurity-induced localized waves in nonlinear lattices

Gaokun Yu, Xinlong Wang,* and Zhiyong Tao
Key Laboratory of Modern Acoustics (MOE) and Institute of Acoustics, Nanjing University, Nanjing 210093, China
(Received 12 August 2010; revised manuscript received 30 November 2010; published 28 February 2011)

We propose a mechanism for soliton creation from resonantly excited localized waves via supratransmission in band gaps of nonlinear lattices. A nonlinear localized wave, which is formed by and vibrates around an impurity with an intrinsic frequency, is found to undergo a local resonance when subject to an external forcing. Under the resonance, an instability develops that leads to the efficient emission of solitons at a much lower rate than that in uniform lattices with no impurity.

DOI: 10.1103/PhysRevE.83.026605 PACS number(s): 05.45.Yv, 43.25.Rq, 47.35.Fg, 42.65.Tg

I. INTRODUCTION

With a fairly good understanding of the soliton properties in regard to their existence, propagation, and interactions [1], creation of solitons has become a central topic in soliton physics, not only fundamental to understanding occurring solitonic phenomena in nature [2–4] and physical systems [5–12], but also very relevant to engineering applications of solitons [13–15]. Although solitons in integrable systems can in principle be evolved from properly given initial disturbances [16], it seems rather problematic to precisely control and realize the initial waveforms that would *definitely* evolve into what we desire. In particular, in real physical systems that are usually nonintegrable, the involvement of other physical effects, including noisy fluctuation, dissipation, and coupling interactions with ambient wave modes, would generally make the precise control of initial conditions extremely difficult or even impossible. Then it necessitates the development of approaches that are practically realizable for efficient creation of solitons.

One of the major approaches, proposed by Friedland *et al.* [17,18] for continuous nonlinear wave systems, was based on a mechanism of autoresonance. In that approach a weak forcing with varying frequency and a specially designed spatial distribution was used to drive a nonlinear wave system through an ensemble of resonances and direct nonlinear waves evolving into large-amplitude solitons. An alternative can be realized by means of the energy supratransmission in band gaps of nonlinear lattices that was discovered by Geniet and Leon [19,20] in nonlinear discrete systems. The mechanism responsible for the energy emission within a band gap was believed [21] to be due to the intrinsic instability of evanescent waves stirred up directly by a boundary drive. Unlike the former, this approach simply uses a *local* drive at a boundary as a source of the transmission, making it quite feasible and manageable in practice. So far, a number of interesting studies have been conducted to explore the existence of the supratransmission phenomenon in other nonlinear systems including optical waveguide arrays [22], Fermi-Pasta-Ulam (FPU) nonlinear chains [23], and nonlinear transmission lines [24,25]. Also, numerical simulations showed the possibility of extending the concept of nonlinear supratransmission to spaces of more than one dimension [26–28].

In this work we propose creation of solitons from a *resonant localized wave* that is induced by an impurity, a scheme that is relevant to but somewhat different from what was uncovered by Leon *et al.* [19–21]. Unlike an evanescent wave stirred up by a boundary drive, an impurity-induced localized wave [29,30] is a kind of intrinsic bound-state wave mode that also is evanescent away from the impurity site but vibrates around the site with an intrinsic frequency ω_r. When subject to an external driving, the localized oscillatory mode can be captured into resonance if the driving frequency ω coincides with the linear frequency ω_r. We observe the supratransmission of a train of solitary waves emitted from the resonant localized wave. By the local resonance, a much smaller drive amplitude is needed to have the input energy be resonantly absorbed by the localized mode. When the stored energy in the localized wave is large enough, part of it is given off as a well-profiled large-amplitude soliton traveling away via supratransmission in band gaps. Another noteworthy feature is that the duration of the resonant absorption and emission, depending on the driving strength, can be so much longer that solitons can be emitted at an extremely low rate as compared to that without an impurity [19]. In one aspect, the soliton emission in this way bears a close resemblance to the stimulated emission, a common phenomenon in physics.

We first in Sec. II discuss the linear properties of the localized wave, which bears a close resemblance to a spring-mass system in classic mechanics. Then in Sec. III we analyze the stationary nonlinear solutions of the localized wave and its instability leading to the emission of solitons. In Sec. IV we numerically investigate in detail the properties of the process of resonant absorption of energy and emission of solitons. Finally, in Sec. V, the present work is concluded.

II. IMPURITY-INDUCED LOCALIZED MODES

We substantiate our idea by using a semi-infinite β-FPU nonlinear chain in which the displacement u_n of the nth particle is governed by

$$m_n\ddot{u}_n = k_2(u_{n+1}+u_{n-1}-2u_n) + k_4[(u_{n+1}-u_n)^3-(u_n-u_{n-1})^3], \quad n=0,1,2,3,\ldots \tag{1}$$

with the double dots over u_n denoting in the usual sense the second derivatives with respect to time t, and k_2 and k_4 being the elastic constants characterizing linear and third-order

*xlwang@nju.edu.cn

nonlinear interactions of neighboring particles. Since both k_2 and k_4 in Eq. (1) can be scaled out by a simple transform of variables, it is assumed that $k_2 = \frac{1}{4}$ and $k_4 = \frac{1}{96}$ in what follows. In the model equation, u_{-1} serves as a displacement drive, and the masses of particles take the values as

$$m_n = \begin{cases} m < 1, & \text{for } n = N \\ 1, & \text{for } n \neq N, \end{cases} \tag{2}$$

meaning an impurity on the Nth site in an otherwise homogeneous semi-infinite lattice.

By letting $u_{-1} = 0$ and linearizing Eq. (1), we can easily obtain the linear solution for the free motion induced by an impurity, which takes the general form [29,31]

$$u_n = (-1)^n a e^{-\kappa|n-N|} e^{-j\omega t} + \text{c.c.}, \quad (N \geqslant 0), \tag{3}$$

with a decaying exponent $\kappa = \kappa_r$ and an intrinsic frequency $\omega = \omega_r$, where "c.c." denotes the complex conjugate of preceding terms. For $N = 0$, it is easily to work out that

$$\kappa_r = \ln \frac{1 - m + \sqrt{1-m}}{m}, \tag{4}$$

$$\omega_r = \frac{1}{2\sqrt{m}} \sqrt{1 + \frac{1}{\sqrt{1-m}}}. \tag{5}$$

It is clear that the linear solution (3) is localized if and only if $m < \frac{3}{4}$. As $m \uparrow \frac{3}{4}$, $\omega_r \downarrow 1$, and $\kappa_r \downarrow 0$, so that ω_r approaches the upper bound of the phonon band from above, and the wave becomes nonlocal. For $N > 0$, ω_r is the root of the eigenvalue equation,

$$\left(\omega_r - \sqrt{\omega_r^2 - 1}\right)^{4(N+1)} + \frac{\sqrt{1-\omega_r^{-2}}}{1-m} = 1, \tag{6}$$

and κ_r is determined by $\omega_r = \cosh \frac{\kappa_r}{2}$. In the limit $N \to \infty$, $\omega_r \to 1/\sqrt{m(2-m)}$, the linear vibration frequency of the impurity mode in an unbounded chain. Figure 1 depicts how ω_r depends on impurity mass m for different locations of impurity.

Now let the chain be driven harmonically by a displacement drive at site $n = -1$,

$$u_{-1}(t) = -2\gamma \cos \omega t = -\gamma e^{-j\omega t} + \text{c.c.}, \tag{7}$$

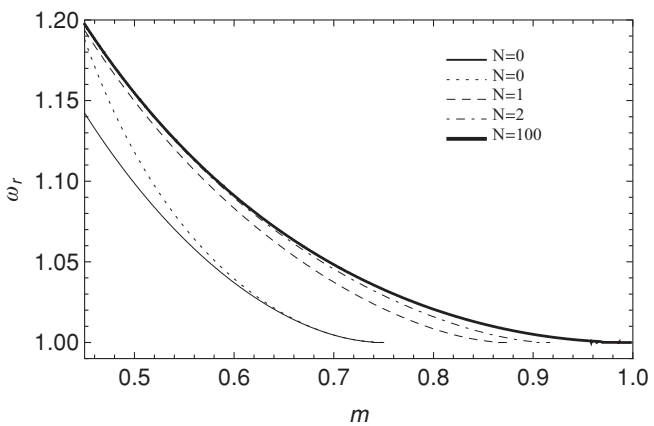

FIG. 1. m dependence of ω_r for different N. The dotted line is the resonant frequency ω_r obtained from the linearized Eqs. (10) and (11) by omitting all nonlinear terms.

whose amplitude $\gamma > 0$ and frequency ω is lying just above the linear phonon band; i.e., $\omega > 1$. For $N = 0$, the stationary solutions of the linearized localized wave assume the form as same as (3), but with a stationary response given by

$$\frac{a}{\gamma} = -\frac{\omega^{-2}}{\omega^{-2} - \omega_r^{-2} - 2\left(\sqrt{1-\omega^{-2}} - \sqrt{1-\omega_r^{-2}}\right)}, \tag{8}$$

$$\begin{cases} <0, & 1 < \omega < \omega_r \\ =\infty, & \omega = \omega_r \\ >0, & \omega > \omega_r \end{cases}.$$

What is clearly seen is the resonance that can occur at $\omega = \omega_r > 1$. Below the resonant frequency, i.e., $1 < \omega < \omega_r$, the local excitation in the vicinity of the impurity vibrates in phase with the drive at site $n = -1$, while above ω_r it is 180° out of phase. The in-phase solution is identified to be purely induced by the impurity; as the impurity becomes light, i.e., $m \downarrow 0$, $\omega_r \to \infty$, and we have $a/\gamma < 0\ \forall \omega \geqslant 1$.

III. NONLINEAR SOLUTIONS AND STABILITIES

The resonant amplification will have the localized wave soon enter into nonlinear motion. We seek its nonlinear solutions in the form

$$u_n(t) = (-1)^n \xi(x,t)|_{x=n} e^{-j\omega t} + \text{c.c.} \tag{9}$$

for $n = 0,1,2,\ldots$. In the way similar to others [32], we assume that the wave oscillates just above the cutoff frequency, i.e., $\omega^2 = 1 + \text{O}(\epsilon^2)$, with ϵ being a parameter measuring the smallness, and it is weakly nonlinear and slowly varies both in time t and in space x along the lattice, so that the wave amplitude $\xi(x,t) = \text{O}(\epsilon)$, $\partial\xi/\partial x = \text{O}(\epsilon)^2$, and $\partial\xi/\partial t = \text{O}(\epsilon)^3$. Substituting Eqs. (7) and (9) into Eq. (1) and performing the long-wave approximation, we can derive, at the cubic order of ϵ, the following equation:

$$-2j\omega \frac{\partial \xi}{\partial t} + \frac{1}{4}\frac{\partial^2 \xi}{\partial x^2} + \frac{1}{2}|\xi|^2 \xi - (\omega^2 - 1)\xi = 0, \tag{10}$$

which governs the evolution of the envelope $\xi(x,t)$, along with the boundary condition

$$8j\omega m \frac{\partial \xi}{\partial t} = (3 - 4m\omega^2)\xi + \frac{\partial \xi}{\partial x} + \frac{1}{2}\frac{\partial^2 \xi}{\partial x^2} + |\xi|^2 \xi + \frac{1}{8}|\gamma + \xi|^2(\gamma + \xi) + \gamma + \text{o}(\epsilon^3), \tag{11}$$

at $x = 0$, if the impurity is located at $N = 0$. Note that in deriving Eq. (11), it is implied that $\gamma = \text{O}(\epsilon)$. Equation (10), which is a nonlinear Schrödinger equation, admits two stationary localized nonlinear solutions [1,31],

$$\xi_\pm(x) = \pm a\, \text{sech}\kappa(x - x_0), \quad (\kappa = a), \tag{12}$$

where x_0, the peak position of the solitary wave, is determined by adapting the solution to the boundary condition (11) and

$$a = 2\sqrt{\omega^2 - 1}, \tag{13}$$

a typical amplitude-frequency response for a nonlinear "hard-spring" system.

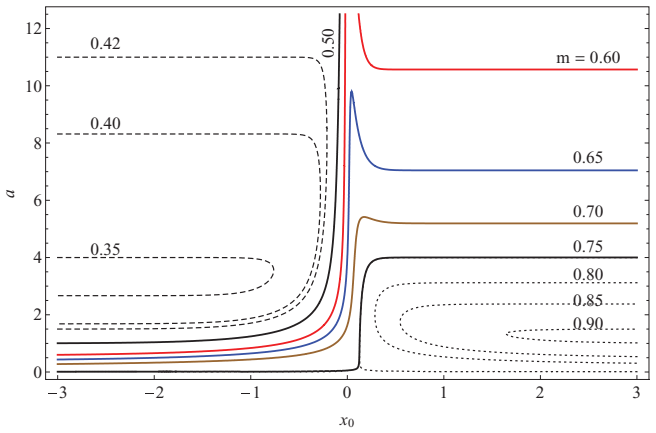

FIG. 2. (Color online) x_0 dependence of the amplitude of the nonlinear free motion of the localized wave: a versus x_0, with the impurity located at $N = 0$ having different masses m as labeled on the curves of different styles [33].

For free motion ($\gamma = 0$), the boundary condition (11) yields the relationship between amplitude a and peak position x_0,

$$a \tanh(a x_0) = 4 \pm \sqrt{5(8 + a^2) - 8m(4 + a^2)}, \qquad (14)$$

which is graphically depicted in Fig. 2, where it is shown that the localized nonlinear solution can be sustained $\forall m < 1$, in contrast to the linear solution, which exists in a smaller range, $m < \frac{3}{4}$. The impurity mass lying within $\frac{1}{2} < m < \frac{3}{4}$, perhaps, is most significant. As shown in Fig. 2, for m taking a value in this range, a is a single-valued function of x_0, and its value can be quite large or even approaches infinity as $m \downarrow \frac{1}{2}$, as long as the envelope is situated inside the chain ($x_0 > 0$). This implies that the localized mode acting as an energy buffer can store a large amount of energy. For $m = 1$, no solution to Eq. (14) does exist, further verifying the nonexistence of the localized nonlinear mode in a uniform chain.

For the displacement-driven nonlinear motion ($\gamma \neq 0$), x_0 is a function of the driving parameters (γ,ω), which can be derived from the boundary condition (11). Figure 3 shows how x_0 depends on γ for several different ω, with solutions ξ_+ in the solid line style and ξ_- in the dashed. Note that for $\omega < \omega_r$, there exists only the ξ_- solution, i.e., the thickest dashed curve in Fig. 3(a), which is identified as induced merely by an impurity, in agreement with the linear result discussed above. This solution also exists for $\omega > \omega_r$, owing to the typical "hard spring" effect of the nonlinear lattice as stated above. As shown in the figure, either of ξ_+ and ξ_- has two branches, one (labeled by "I" for ξ_+, by "III" for ξ_-) being monotonically increasing with x_0, and the other (labeled by "II" for ξ_+, "IV" for ξ_-) monotonically decreasing with x_0. By contrast, only the ξ_+ solution exists in the case of no impurity, whatever the driving frequency ω is, as can be seen from the corresponding x_0 versus γ dependence shown in Fig. 3(b). And, because of the absence of resonant amplification mechanism in this case, larger γ is needed in order to support a stationary evanescent wave at the boundary.

A linear perturbation analysis [34,35] for solutions (12) reveals that branch "I" of ξ_+ is linearly stable. On the contrary, branches "II" and "IV" are always unstable, hence irrealizable both numerically and physically. Branch "I", which exists even in the case of no impurity, can be made unstable by a saddle-node bifurcation only if γ exceeds a threshold, i.e., the peak γ value in Fig. 3(b). This is the fundamental instability that leads to the supratransmission, as already discussed by Leon *et al.* [21]. In the present situation, we observe through numerical simulations that the instability usually leads branch "I" to transit to branch "III." The stability of branch "III" of the impurity-induced solution ξ_-, however, is quite different. By solving the eigenvalue λ of the perturbation problem, we have calculated the growth rate Re(λ) of an infinitesimal disturbance on ξ_-, which depends highly on the driving amplitude γ as shown in Fig. 4(a). On can find that for γ greater than a threshold γ_c for a given ω, $0 < \mathrm{Re}(\lambda) \ll 1$, implying an instability development at an *extraordinarily low speed*. The stability also is examined by direct numerical simulations, yielding the consistent results as shown in Fig. 4(b). In the long-term instability development, the resonantly localized mode ξ_- will absorb a large amount of energy from the drive as the stored localized energy, which will finally be emitted in the form of large-amplitude solitons, as shown in Fig. 5.

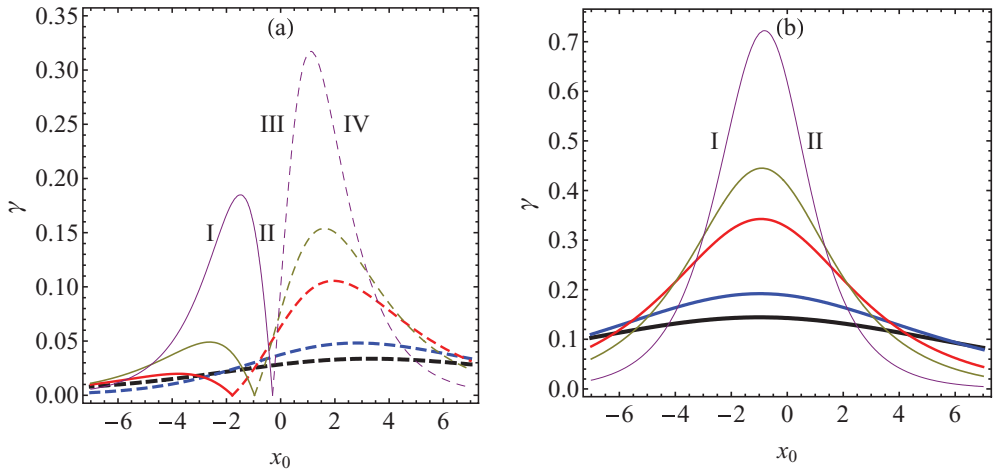

FIG. 3. (Color online) γ dependences of the peak position x_0 for (a) $m = 0.7$ and (b) $m = 1$. In (a), the solid lines are for the solution ξ_+ and the dashed for ξ_-. In the case of $m = 1$, only the ξ_+ solution exists. Every curve is calculated for a fixed $\omega = \omega_r + \Delta\omega$, with an offset $\Delta\omega$ taking value, from the thickest curve to the thinnest, -0.002, 0, 0.01, 0.02, and 0.06.

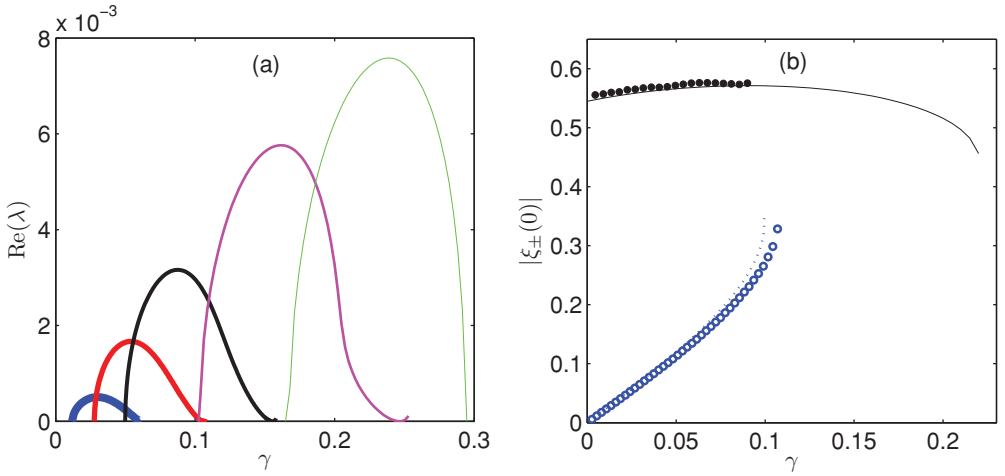

FIG. 4. (Color online) (a) The growth rate Re(λ) versus γ for branch "III" calculated for a fixed $\omega = \omega_r + \Delta\omega$, with an offset $\Delta\omega$ taking a value, from the thickest curve to the thinnest, 0.002, 0.01, 0.02, 0.04, and 0.06. (b) The numerically computed amplitude of branch "I" (the empty circles) and "III" (the filled circles), along with their theoretical predictions (the thin dotted line for "I" and thin solid line for "III"), all with $\omega = 1.04$. (It is assumed here that $N = 0$ and $m = 0.7$ ($\omega_r \approx 1.0046$).

IV. PROPERTIES OF THE SOLITON EMISSION

Intensive numerical investigations have been performed to go into the details of the creation of solitons from resonantly excited localized waves and the differences of the resonant emission from the case of no impurity. To avoid the possible formation of sudden shocks [23] in our simulation, the driving amplitude increases smoothly form zero to a constant value as $\gamma[1 - \exp(-t/\tau_1)]$, with τ_1 being set 500. Since only a finite chain is manageable by a computer, we add viscous terms, $\nu_n \dot{u}_n$, on the left-hand sides of Eq. (1) for a number of sites on the far end of the chain, so as to minimize the reflection from the end [20]. Then Eq. (1), together with the initial conditions, $u_n(0) = \dot{u}_n(0) = 0$, is numerically solved by the forth-order Runge-Kutta algorithm of variable step size.

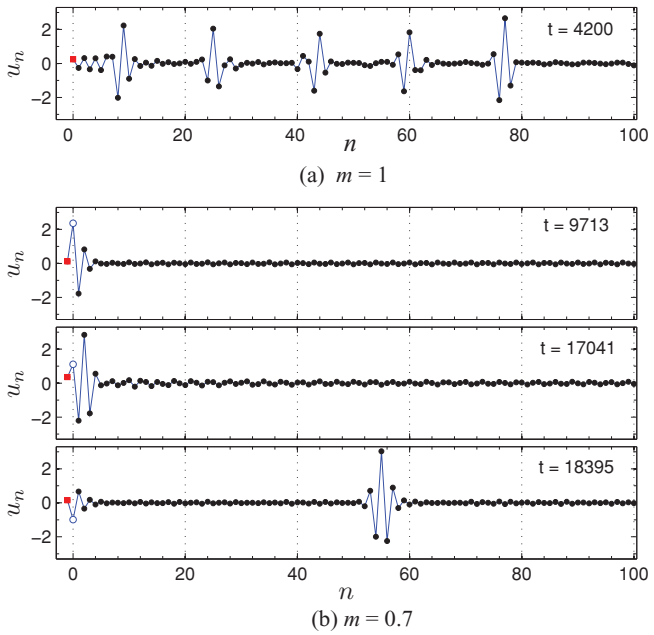

(a) $m = 1$

(b) $m = 0.7$

FIG. 5. (Color online) (a) Snapshot of soliton emission (at $t = 4200$) in a chain without an impurity for $\gamma = 0.611$. (b) Snapshots of the resonant emission (at thee different instants as labeled) from the localized wave induced by an impurity at location $N = 0$ (the empty circle) and driven by a displacement source (the filled square) of amplitude $\gamma = 0.206$. In both cases, the driving frequency $\omega = \omega_r + 0.04$, and the plots show only the first 100 sites of the vibratory chain of total 800 sites.

Figure 5, as a typical example, shows the difference of the emissions for (a) with no impurity and (b) with an impurity of mass $m = 0.7$ at the site of $N = 0$. In the former case ($m = 1$), only for a sufficiently large driving amplitude γ, say, $\gamma = 0.611$ here, does the agitated evanescent wave develop its instability and emit solitonic pulses. Because the evanescent wave is incapable of buffering energy, solitons are emitted one after another rapidly. By contrast, in the latter case, even a quite small driving amplitude, say, $\gamma = 0.206$, can have the localized wave resonantly amplified to an amplitude a so large that solitons emission occurs. In this example, the impurity-induced localized wave has an intrinsic frequency $\omega_r = 1.0046$ in small-amplitude vibration, and the driving frequency ω is set to be slightly higher than ω_r, with a detuning of 0.04. Since the impurity-induced localized wave acts like a mechanical oscillator, it has the capacity of storing and buffering energy absorbed from the driving source, in particular, under resonance. Of course, for such a weak drive (small γ), this process of energy absorption and storage will take a much longer time before the absorbed energy is large enough to give off a large-amplitude envelope soliton. The remarkably different rates of emissions, with and without an impurity, can be read more clearly from the time domain waveforms shown in Fig. 6.

The threshold γ_c, the minimal γ that is required for initiating the emission of solitons, depends on driving frequency ω, as well as other parameters, especially the impurity mass m and its position N. Figure 7(a) presents our numerically computed γ_c versus ω for an impurity of $m = 0.7$ located at different sites N. It is seen that, for $N = 0$, the nearest site to the drive, γ_c is significantly lower than that with no impurity. With

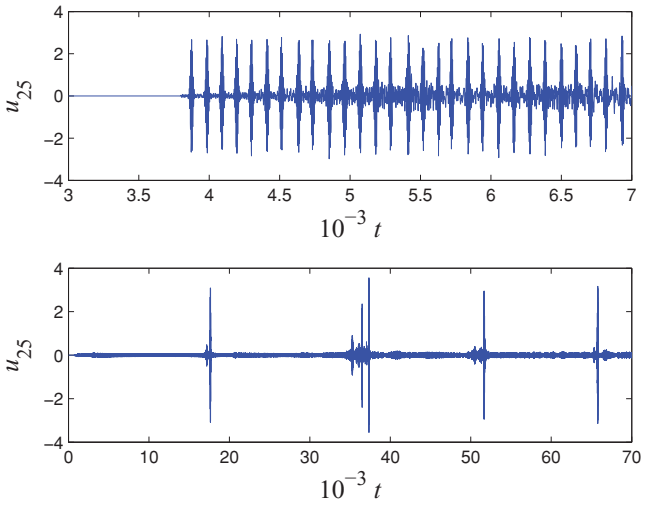

FIG. 6. (Color online) Time domain waveforms at site $n = 25$ for (a) $m = 1$ and (b) $m = 0.7$ and $N = 0$. The driving parameters are as same as in Fig. 5.

the impurity located far away from the drive (large N), large threshold γ_c is needed in general, not only because of the higher linear resonant frequency ω_r, as is shown in Fig. 1, but also because of the less efficiency of coupling the input energy into the localized mode. In fact, the impurity plays little role in the generation of solitons if $N \geqslant 5$, and soliton emission is essentially as same as that without an impurity [21].

For an impurity of mass $m = 0.8$, the situation is a little different, since in the linear case the impurity-induced wave is nonlocal for $N = 0$, and there is no associated linear resonance as well, as can be seen in Fig. 1. Only for $N \geqslant 1$ is the impurity-induced wave localized with an eigenfrequency ω_r. In the nonlinear case, nevertheless, the impurity-induced wave motion may, as already implied in Fig. 2, become localized and be entranced into nonlinear resonance, and yet soliton creation is possible at a small γ. In fact, we observe no evident difference between the amplitude thresholds for the cases $N = 0$ and 1, as is shown in Fig. 7(b). A direct comparison is presented in Fig. 7(c) of the driving threshold γ_c for different masses, all located at $N = 0$. It more clearly illustrates how the nonlinear resonance results in soliton emissions at a remarkably lower threshold γ_c.

It is observed that the duration (period) T between two emissions on average is highly sensitive to the driving parameters (ω, γ). Figure 8 presents the γ dependence of the average period T for different detuning $\Delta\omega = \omega - \omega_r$ in the log-log plots. It is shown that $10^3 < T < 10^5$, which means a very low emission rate T^{-1}, consistent with the prediction by

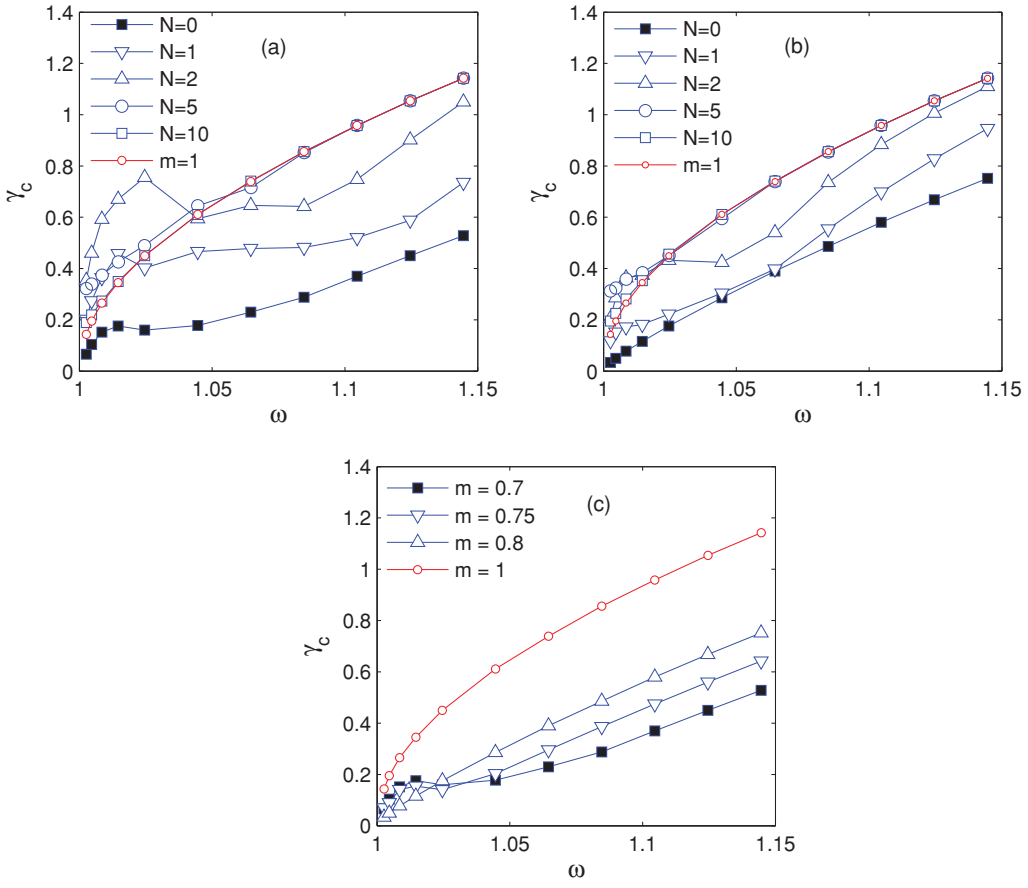

FIG. 7. (Color online) Threshold γ_c versus ω for impurities positioned at different sites N. (a) $m = 0.7$, with resonant frequencies $\omega_r \approx 1.0046, 1.0374$, and 1.0455, respectively, for $N = 0, 1$ and 2; (b) $m = 0.8$ with resonant frequencies $\omega_r \approx 1.0085$ and 1.0159, respectively, for $N = 1$ and 2; (c) for the site $N = 0$ with m taking different values. The curves for $m = 1$(the homogeneous chain) are also included for comparison.

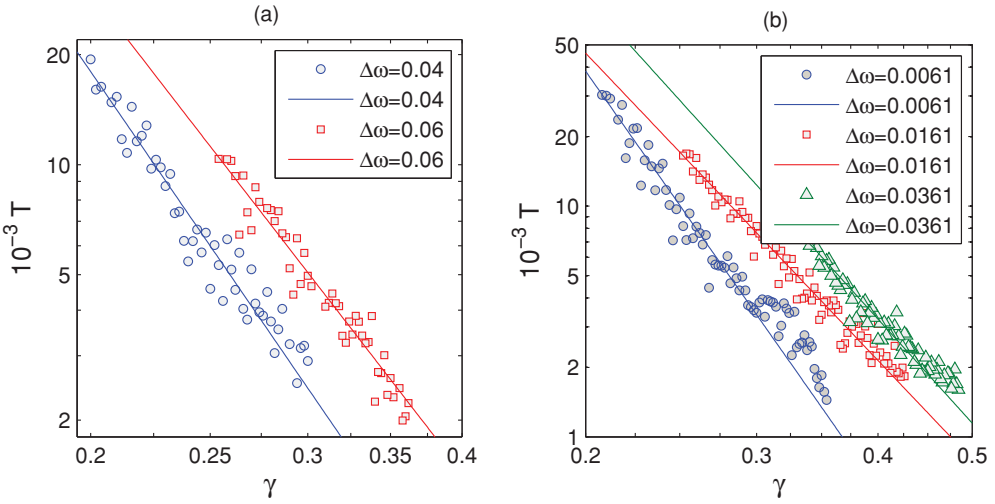

FIG. 8. (Color online) Average emission period T versus γ for the impurities: (a) $m = 0.7$ ($\omega_r \approx 1.0046$) located at $N = 0$, and (b) $m = 0.8$ ($\omega_r \approx 1.0085$) at $N = 1$. In the legends, $\Delta\omega \equiv \omega - \omega_r$. The different data sets in different symbols are for different detuning $\Delta\omega$, and the solid line around each data set is the best fitting by the formula $T = T_1\gamma^{-b}$, with $(T_1,b) \approx (6.537,4.921)$ and $(26.48,4.364)$, respectively, for $\Delta\omega = 0.04$ and 0.06 in (a), and $(T_1,b) \approx (2.469,5.998),(37.09,4.427)$ and $(45.79,4.648)$, respectively, for $\Delta\omega = 0.0061,0.0161$, and 0.0261 in (b).

the growth rate shown in Fig. 4. The data can well be fitted by $T = T_1\gamma^{-b}$, with T_1 and b both positive. As $\gamma \downarrow \gamma_c$, the resonant localized wave gives off solitons at an extremely low rate.

Once a soliton is generated, it travels along the chain at speed c. A traveling soliton also governed by Eq. (10) has the following solution:

$$\xi(x,t) = a\,\mathrm{sech}[a(x - ct - x_0)]\,e^{i(-kx+\phi_0)}, \tag{15}$$

with x_0 and ϕ_0 being arbitrary constants, and $k = 4c\omega$. Now instead of formula (13), the amplitude a is given by $a = \sqrt{4(\omega^2 - 1) + k^2}$, and it is directly related to soliton speed c. We observe that at the instant a soliton is emitted from the localized wave, the wave envelope will increase its amplitude a a little, and it then starts propagating at a constant speed c. This is consistent with the theoretical prediction.

To examine the efficiency with which to generate solitons, consider the local energy flux

$$\bar{j}_n = \frac{1}{\Delta t}\int_t^{t+\Delta t} \frac{du_n}{dt}[k_2(u_n - u_{n+1}) + k_4(u_n - u_{n+1})^3]dt, \tag{16}$$

averaged over a time interval Δt both at the input $n = -1$ and at a site inside the chain, say, $n = 25$, which is so much away from the driving end (or the impurity) that the evanescent or localized wave is negligible there but is close enough to ensure that there is no additional traveling solitons. Here Δt that we use should, in principle, be the period $2\pi/\omega$ of the dominant oscillation, but here we would rather use a longer interval that is multiple times the period, so as to minimize the effect due to random background fluctuation. The input energy E_{in} and the energy E_{25} passing through the 25th site are calculated from $\bar{j}_{-1}$ and $\bar{j}_{25}$ simply by quadrature, respectively. Figure 9 shows the energies, as well as their difference $E_{\mathrm{local}} = E_{\mathrm{in}} - E_{25}$, for two cases: (a) without an impurity and (b) with an impurity. Here E_{local} well approximates the local energy that is stored in the evanescent wave in the vicinity of the drive (or in the localized wave if an impurity is present). When E_{local} accumulates to an upper level, $\max(E_{\mathrm{local}})$, a soliton is emitted and E_{local} drops back to a lower level, $\min(E_{\mathrm{local}})$. Hence, the energy E_{soliton} carried away with a traveling soliton can be approximated by $E_{\mathrm{soliton}} \approx \max(E_{\mathrm{local}}) - \min(E_{\mathrm{local}})$. We therefore can measure the efficiency of soliton emission by

$$Q = \frac{E_{\mathrm{soliton}}}{\max(E_{\mathrm{local}})} = 1 - \frac{\min(E_{\mathrm{local}})}{\max(E_{\mathrm{local}})}, \tag{17}$$

which is the ratio of the energy carried with a single soliton to the input energy during one period T of soliton emission. In the absence of an impurity, we see that soliton creation is possible only if E_{local} first is built up beyond a minimum level, $\min(E_{\mathrm{local}})$, which seems remarkably high. From the data displayed in Fig. 9(a), it is estimated that $Q \approx 49\%$, showing that most input energy is trapped in the vicinity of the drive. By contrast, in the presence of an impurity, an emitted soliton carries almost all energy accumulated in the localized wave, and E_{local} drops back to a level, $\min(E_{\mathrm{local}})$, that is almost vanishing. It is estimated from Fig. 9(b) that $Q \approx 90\%$, showing that soliton creation from a resonant localized wave is more efficient.

A. Remarks

We have noted in our simulations that the localized wave may occasionally cease or stop emitting after giving off a few solitons. This phenomenon is caused presumably by the weak reflection from the far end, although much of the reflection is damped out by introducing the damping on the farthest sites, as described at the beginning of this section. The argument is verified by the fact that the longer (more sites) the nonlinear chain is, the later the emission terminates. We find from our simulations that a better way to prevent the emission halt is imposing a weak damping on the impurity particle, that is,

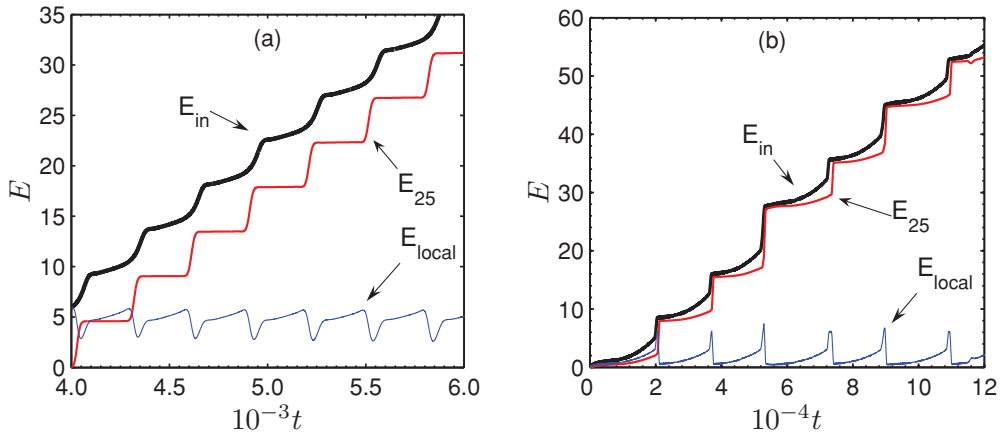

FIG. 9. (Color online) Time variations of input energy ($E_{\rm in}$), transport energy (E_{25}) through site $n = 25$, and the energy difference ($E_{\rm local} = E_{\rm in} - E_{25}$) for two cases: (a) without an impurity ($m = 1, \gamma = 0.345$) and (b) with an impurity ($m = 0.8, N = 1, \gamma = 0.234$, $\omega_{\rm r} \approx 1.0085$), In both cases, $\omega = \omega_{\rm r} + 0.0061$.

adding a damping term, $\nu_N \dot{u}_N$, to the equation of motion for the impurity site $n = N$ in Eq. (1), with a damping coefficient ν_N of the order as small as $10^{-5} \sim 10^{-2}$.

Interestingly, we also find that damping imposed on the impurity particle can even make emitted waves more regular and well profiled as solitons, an extra favorable effect on creation of solitons. Presented in Fig. 10 is an extreme example

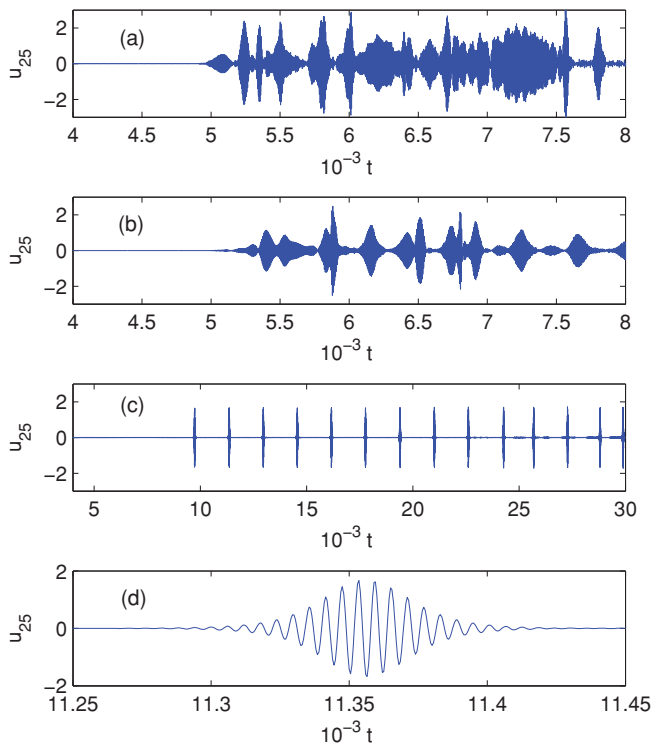

FIG. 10. (Color online) Time-domain waveforms of emitted waves at site $n = 25$ for a damped impurity of mass $m = 0.8$ located at $N = 0$ and excited at frequency $\omega = 1.0446$, with (a) $\gamma = 0.2846$ and $\nu = 0$, (b) $\gamma = 0.2852$ and $\nu = 0.01$, and (c) $\gamma = 0.3187$ and $\nu = 0.08$. (d) The enlarged portion by stretching the abscissa of (c), so as to make it easily viewable the detail of the second pulse in (c).

that shows that (a) the emitted waves would appear turbulence-like at a large driving amplitude, say, $\gamma = 0.2852$, but (b) the situation is made significantly changed by introducing the damping effect, and (c) in particular, with a reasonably large damping coefficient, say, $\nu = 0.08$, the turbulence-like behaviors are depressed altogether and instead solitonic pulses are given off from the localized wave at a constant rate. The emitted pulses, whose detailed profile can be more clearly seen in the stretched plot in Fig. 10(d), appear to be some standard nonlinear Schrödinger solitons passing through the detecting site at $n = 25$. Of course, a little greater γ is needed to balance the damping dissipation.

V. CONCLUSIONS AND DISCUSSION

In summary, we have proposed a mechanism of soliton creation from resonantly excited localized waves in nonlinear lattices. Since a localized wave, which can be formed by introducing an impurity in otherwise homogeneous nonlinear lattices, is an standing oscillatory mode behaving essentially like a classical oscillator with its own intrinsic frequency $\omega_{\rm r}$, it will resonate with an external drive when the driving frequency ω is in proximity to $\omega_{\rm r}$. It was shown that the nonlinear resonance will make the localized wave unstable, leading to its emission of solitons, which appears quite different from that by directly driving a uniform nonlinear systems without an impurity.

One of the distinct features with the present method is that the resonance makes it possible to create solitons at very weak driving strength γ by slow absorption and accumulation of input energy, which might be useful in practical realizations. Another interesting feature is that solitons can be created at a much lower rate, which appears to be highly adjustable with the driving parameters, implying the feasibility of precisely controlling the creation.

It seems straightforward to extend the mechanism of soliton creation to general nonlinear systems. For example, we have confirmed (but omitted in this paper) that the emission of solitons from resonant localized waves in a discrete sine-Gordon nonlinear chain of coupled oscillators can be realized

in much wider ranges of driving parameters [19], and in particular, it seems more efficient than by simply driving a boundary site without an impurity.

ACKNOWLEDGMENTS

We would like to acknowledge the support of the NSFC under Grant No. 10874085.

[1] M. Remoissenet, *Waves Called Solitons: Concepts and Experiments* (Springer, New York, 1999).
[2] R. Trines, R. Bingham, M. W. Dunlop, A. Vaivads, J. A. Davies, J. T. Mendonca, L. O. Sil, and P. K. Shukla, Phys. Rev. Lett. **99**, 205006 (2007).
[3] D. Farmer and L. Armi, Science **283**, 188 (1999).
[4] G. M. Reznik and V. Zeitlin, Phys. Rev. Lett. **96**, 034502 (2006).
[5] J. Wu, R. Keolian, and I. Rudnick, Phys. Rev. Lett. **52**, 1421 (1984).
[6] J. Denschlag, J. E. Simsarian, D. L. Feder *et al.*, Science **287**, 97 (2000).
[7] K. E. Strecker, G. B. Partridge, A. G. Truscott, and R. G. Hulet, Nature (London) **417**, 150 (2002).
[8] M. Wu, B. A. Kalinikos, and C. E. Patton, Phys. Rev. Lett. **93**, 157207 (2004).
[9] I. Kourakis, N. Lazarides, and G. P. Tsironis, Phys. Rev. E **75**, 067601 (2007).
[10] P. J. Reece, E. M. Wright, and K. Dholakia, Phys. Rev. Lett. **98**, 203902 (2007).
[11] B. Damski and W. H. Zurek, Phys. Rev. Lett. **104**, 160404 (2010).
[12] E. Bourdin, J.-C. Bacri, and E. Falcon, Phys. Rev. Lett. **104**, 094502 (2010).
[13] M. Nakazawa, K. Suzuki, E. Yamada, H. Kubota, Y. Kimura, and M. Takaya, Electron. Lett. **29**, 729 (1993).
[14] A. Hasegawa, Physica D (Amsterdam) **123**, 267 (1998).
[15] H. A. Haus and W. S. Wong, Rev. Mod. Phys. **68**, 423 (1996).
[16] S. Clarke, R. Grimshaw, P. Miller, E. Pelinovsky, and T. Talipova, Chaos **10**, 383 (2000).
[17] L. Friedland and A. G. Shagalov, Phys. Rev. Lett. **81**, 4357 (1998).
[18] L. Friedland and A. G. Shagalov, Phys. Rev. Lett. **90**, 074101 (2003).
[19] F. Geniet and J. Leon, Phys. Rev. Lett. **89**, 134102 (2002).
[20] F. Geniet and J. Leon, J. Phys. Condens. Matter **15**, 2933 (2003).
[21] J. Leon, Phys. Lett. A **319**, 130 (2003).
[22] R. Khomeriki, Phys. Rev. Lett. **92**, 063905 (2004).
[23] R. Khomeriki, S. Lepri, and S. Ruffo, Phys. Rev. E **70**, 066626 (2004).
[24] S. B. Yamgoué, S. Morfu, and P. Marquié, Phys. Rev. E **75**, 036211 (2007).
[25] K. Tse Ve Koon, J. Leon, P. Marquié, and P. Tchofo-Dinda, Phys. Rev. E **75**, 066604 (2007).
[26] J. E. Macías-Díaz, Phys. Rev. E **77**, 016602 (2008).
[27] J. E. Macías-Díaz, Phys. Rev. E **78**, 056603 (2008).
[28] J. E. Macías-Díaz, Commun. Nonlinear Sci. Numer. Simul. **14**, 1025 (2009).
[29] K. Nagahama and N. Yajima, J. Phys. Soc. Jpn. **58**, 1539 (1989).
[30] D. Hennig, K. Ø. Rasmussen, G. P. Tsironis, and H. Gabriel, Phys. Rev. E **52**, R4628 (1995).
[31] Y. S. Kivshar, F. Zhang, and S. Takeno, Physica D **113**, 248 (1998).
[32] N. V. Alexeeva, I. V. Barashenkov, and G. P. Tsironis, Phys. Rev. Lett. **84**, 3053 (2000).
[33] The value of a shown in the figure seems not consistent with the assumption made before, i.e., $\xi = \mathrm{O}(\epsilon)$. Nevertheless, it is quite often in nonlinear physics that many equations of evolution and their solutions that were derived under similar assumptions, typically $\epsilon \ll 1$, by the multiscales technique and perturbation analyses can be extrapolated beyond the assumptions in an asympototic sense. Our numerical simulations, including those in the subsequent sections, have verified the validity of the result presented in this figure, at least qualitatively.
[34] K. W. Sandusky, J. B. Page, and K. E. Schmidt, Phys. Rev. B **46**, 6161 (1992).
[35] D. Bonart, A. P. Mayer, and U. Schröder, Phys. Rev. B **51**, 13739 (1995).